Comparison of Bone Tunnel and Cortical Surface Tendon-to-Bone Healing in a Rabbit Model of Biceps Tenodesis

Hongbo Tan, MD, PhD, Dean Wang, MD, Amir H. Lebaschi, MD, Ian D. Hutchinson, MD, Liang Ying, BS, Xiang-Hua Deng, MD, Scott A. Rodeo, MD, and Russell F. Warren, MD

Investigation performed at the Hospital for Special Surgery, New York, NY

Background: Many orthopaedic surgical procedures involve reattachment of a single tendon to bone. Whether tendon-to-bone healing is better facilitated by tendon fixation within a bone tunnel or on a cortical surface is unknown. The purpose of this study was to evaluate tendon-healing within a bone tunnel compared with that on the cortical surface in a rabbit model of biceps tenodesis.

Methods: Thirty-two rabbits (24 weeks of age) underwent unilateral proximal biceps tenodesis with tendon fixation within a bone tunnel (BT group) or on the cortical surface (SA [surface attachment] group). Postoperatively, rabbits were allowed free-cage activity without immobilization. All rabbits were killed 8 weeks after surgery. Healing was assessed by biomechanical testing, microcomputed tomography (micro-CT), and histomorphometric analysis.

Results: Biomechanical testing demonstrated no significant difference between the groups in mean failure loads (BT: 56.8 ± 28.8 N, SA: 55.8 ± 14.9 N; p = 0.92) or stiffness (BT: 26.3 ± 16.6 N/mm, SA: 32.3 ± 9.6 N/mm; p = 0.34). Micro-CT analysis demonstrated no significant difference between the groups in mean volume of newly formed bone (BT: 69.3 ± 13.9 mm^3, SA: 65.5 ± 21.9 mm^3; p = 0.70) or tissue mineral density of newly formed bone (BT: 721.4 ± 10.9 mg/cm^3, SA: 698.6 ± 26.2 mg/cm^3; p = 0.07). On average, newly formed bone within the tunnel represented only 5% of the total new bone formed in the BT specimens. Histological analysis demonstrated tendon-bone interdigitation and early fibrocartilaginous zone formation on the outer cortical surface in both groups. In contrast, minimal tendon-bone bonding was observed within the tunnel in the BT specimens.

Conclusions: Tendon fixation in a bone tunnel and on the cortical surface resulted in similar healing profiles. For tendons placed within a bone tunnel, intratunnel healing was minimal compared with the healing outside the tunnel on the cortical surface.

Clinical Relevance: The creation of large bone tunnels, which can lead to stress risers and increase the risk of fracture, may not be necessary for biceps tenodesis procedures.

Tendinosis of the long head of the biceps has long been recognized as a possible source of shoulder pain[1,2]. Although the pathomechanism by which it acts as a pain generator in the shoulder is not fully understood, tenodesis of the biceps tendon is commonly performed to address the disease. Many surgeons prefer biceps tenodesis over tenotomy in order to maintain the length-tension relationship of the biceps muscle, thereby preventing cramping, preserving strength, and providing better cosmesis[3,4].

With the evolution of suture anchors, cortical buttons, and interference screws, numerous biceps tenodesis techniques have been described. Most of these surgical constructs have demonstrated excellent time-zero pullout strengths[4-7], with each technique designed to facilitate tendon-to-bone healing through integration within a bone tunnel or on the cortical surface. Advocates for bone-tunnel fixation believe that healing may be enhanced by its allowance of more contact surface area between the tendon and cancellous bone and greater exposure to marrow-derived endogenous stem cells[8-10]. However, the creation of a large cortical hole using this technique can lead to stress concentration, increasing the risk of fracture[11,12]. Furthermore, placement of the biceps tendon in a bone tunnel

Disclosure: No external funding was received for this study. The **Disclosure of Potential Conflicts of Interest** forms are provided with the online version of the article (http://links.lww.com/JBJS/E647).

generates a "killer turn" that positions the tendon orthogonal to the tunnel aperture, which can result in local deformations of the tendon[13,14]. Although techniques that affix the long head of the biceps tendon either within a bone tunnel or on the cortical surface have demonstrated good clinical results[14-16], each has its own specific complication profiles[11,17-20], and it is currently unknown as to which method results in a stronger biological construct. Ultimately, the long-term success of tenodesis likely depends on the integrity of tendon-to-bone healing.

The purpose of the current study was to evaluate tendon-healing within a bone tunnel compared with healing on a cortical surface in a rabbit model of biceps tenodesis. We assessed tendon-to-bone healing at 8 weeks with biomechanical testing, microcomputed tomography (micro-CT), and histomorphometric analysis.

Materials and Methods

Thirty-two skeletally mature, male New Zealand White rabbits (age, 24 weeks; weight, 3.2 to 3.9 kg) were used to evaluate tendon-to-bone healing in a biceps tenodesis model. The rabbits were obtained from a U.S. Department of Agriculture-licensed dealer and were housed in the facility for the care of laboratory animals in accordance with the standards established by the National Institutes of Health. This study was approved by the Institutional Animal Care and Use Committee.

Experimental Design

All animals underwent unilateral tenodesis of the long head of the biceps tendon of the right shoulder. Sixteen rabbits were assigned to each experimental group (bone tunnel [BT] or cortical surface attachment [SA]). Surgeries were performed in a randomized fashion, and all animals were killed at 8 weeks postoperatively. Ten rabbits from each group were prepared for biomechanical testing, 7 of which underwent scanning with use of micro-CT prior to testing. The other 6 rabbits were prepared for histological evaluation.

Surgical Procedure

Animals were anesthetized by the Research Animal Resource Center staff with use of intramuscular ketamine hydrochloride (50 mg/kg) and midazolam (4 mg/kg) and maintained on inhalation anesthesia (isoflurane, nitrous oxide, and oxygen). Intramuscular penicillin G procaine (150,000 units) was administered for infection prophylaxis. The deltopectoral approach was used to expose the humerus. The rotator interval was opened, and a 5-mm segment of the biceps tendon was marked in situ at the level of the surgical neck, where the suprapectoral tenodesis was performed. This was done to maintain the native length-tension relationship of the biceps. The biceps origin at the superior part of the glenoid was then sharply released, and the bicipital groove was exposed. For fixation in the BT group, a single tunnel measuring 2.4 mm in diameter was drilled unicortically within the bicipital groove, to a depth of 5 mm. Through this created tunnel, a 1.1-mm hole was then drilled, exiting the lateral humeral cortex. A locking whipstitch using 2-0 Ethibond suture (Ethicon) was placed through the proximal end of the tendon. The suture ends were shuttled through the tunnel and out the lateral

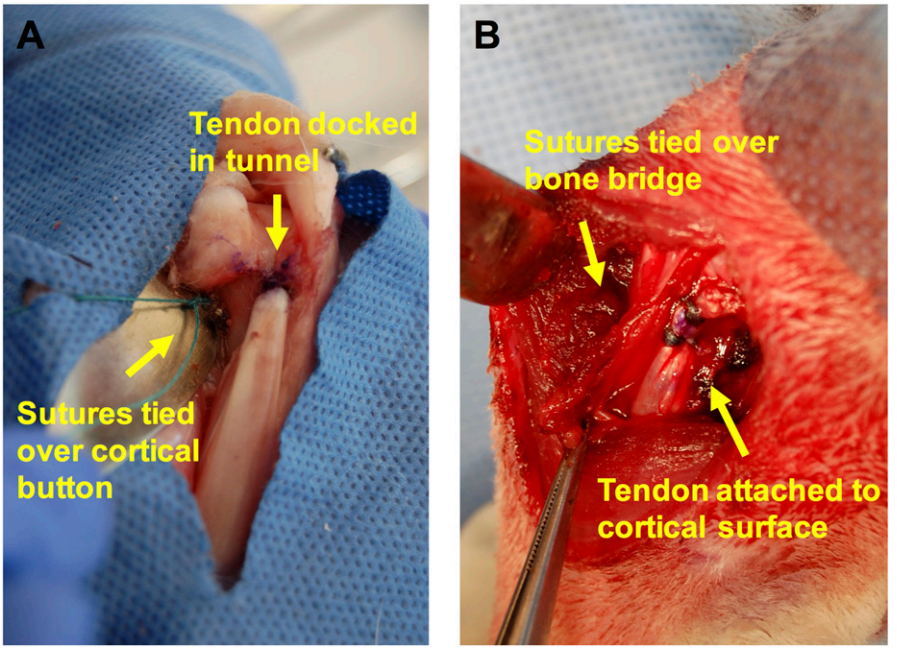

Fig. 1

Proximal biceps tenodesis with tendon fixation within a bone tunnel (**Fig. 1-A**) or on the cortical surface (**Fig. 1-B**). **Fig. 1-A** The biceps tendon is docked within a bone tunnel 2.4 mm in diameter and secured with sutures tied over a cortical button for suspensory fixation. **Fig. 1-B** Two modified Kessler sutures are placed in the proximal end of the biceps tendon, shuttled through drill holes to the lateral cortex, and tied over a bone bridge.

TABLE I Histomorphometric Scoring Criteria for the Assessment of Fibrocartilage Zone Formation at the Tendon-Bone Interface*

Characteristic	Score
Fibrocartilage zone formation	
None (0% of interface)	0
Slight (<50% of interface)	1
Moderate (>50% of interface, average thickness <100 μm)	2
Substantial (>50% of interface, average thickness 100-200 μm)	3
Massive (>50% of interface, average thickness 200-500 μm)	4
Excellent (100% of interface, average thickness >500 μm)	5
Tendon bonding to adjacent tissues	
0% of interface	0
<25% of interface	1
25%-49% of interface	2
50%-74% of interface	3
75%-99% of interface	4
100% of interface	5

*Table data from Zhou et al.[21].

cortex, and the 5-mm marked portion of tendon was docked within the medullary canal (Fig. 1-A). The sutures were tied over a metal cortical button on the lateral humeral cortex for suspensory fixation (Fig. 1-A). For fixation in the SA group, the cortical surface within the bicipital groove was exposed and slightly decorticated with a scalpel, without breaching the cortex. Two sets of parallel, 1.1-mm holes, 5 mm apart, were drilled in a bicortical fashion starting within the groove and exiting the lateral part of the humerus. This created a rectangular pattern of a total of 4 holes within the bicipital groove. Two modified Kessler stitches using 2-0 Ethibond were placed in the 5-mm marked portion of the tendon, resulting in 4 suture limbs. These limbs were then shuttled through the corresponding drill holes and tied over a bone bridge on the lateral cortex (Fig. 1-B). Postoperatively, the rabbits were allowed normal activity in individual cages, without immobilization. Animals were observed twice daily for signs of pain and were given 0.01 to 0.05 mg/kg of Buprenex (buprenorphine) intramuscularly up to twice per day for postoperative analgesia. At 8 weeks, the animals were killed by a dose of intravenous phenobarbital.

Biomechanical Testing

Forequarter limbs were frozen and stored at –80°C until biomechanical testing. At the time of biomechanical testing, the limbs were thawed at room temperature, and all soft tissue except for the attached biceps tendon was removed. Additionally, all suture and cortical buttons were removed, with care taken so as to not violate the tenodesis site. The humerus-biceps tendon complexes were fixed in a custom-designed device allowing tensile loading along the axis of the biceps tendon in a custom Materials Testing machine. The humeral shaft was fixed with a clamp and additionally secured with 2 Kirschner wires. For a set of native biceps-intact specimens, all soft tissue was removed from the scapula, with the exception of the glenoid-biceps tendon complex. The entire scapula was potted in Bondo lightweight filler (3M) and locked in a vise grip. The biceps tendons were cleared of residual muscle and secured in a custom grip oriented along its longitudinal axis. Following 3 cycles of preconditioning to 5 N at a rate of 1 mm/min, a load-to-failure test was performed at an elongation rate of 1 mm/min. Stiffness (N/mm) was calculated from the slope of the linear region of the load-elongation curve. The mode of failure was recorded for each specimen.

Micro-CT

After the animal was killed, the humerus was disarticulated at the elbow joint, and the biceps tendon was detached distally from its radial attachment. Bone morphometry and density were evaluated by micro-CT (Scanco μCT 35; Scanco Medical). Scans were performed at 15-μm voxel size (E = 55 kVp), 0.36° rotation step (180° angular range), and 400-ms exposure per view. Scanning was performed with all specimens placed in Dulbecco phosphate-buffered saline solution. After 3-dimensional reconstruction of the images, contours of newly formed bone on the cortical surface were manually drawn on all slices from 5 mm proximal to 5 mm distal to the center of the attachment site. Additionally, for the BT specimens, cylindrical contours of newly formed bone within the bone tunnel were manually drawn on all slices from the tunnel aperture to a depth of 5 mm. Within these areas of interest (representing total volume), calculations of bone volume, bone

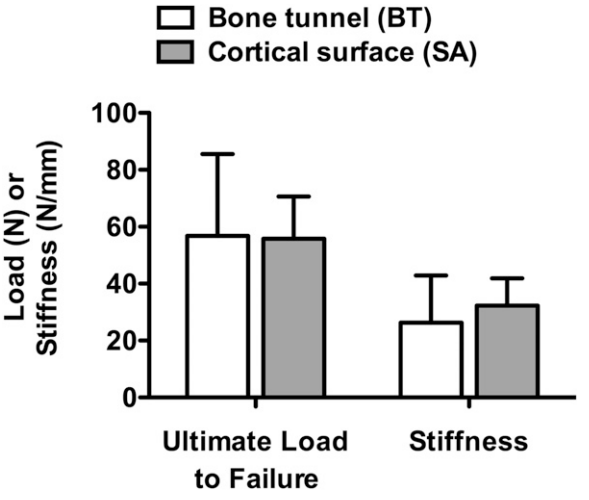

Fig. 2

Results of biomechanical testing of biceps tendon-bone constructs. No significant differences in mean ultimate load to failure or stiffness between the groups was found. The error bars represent the standard deviation.

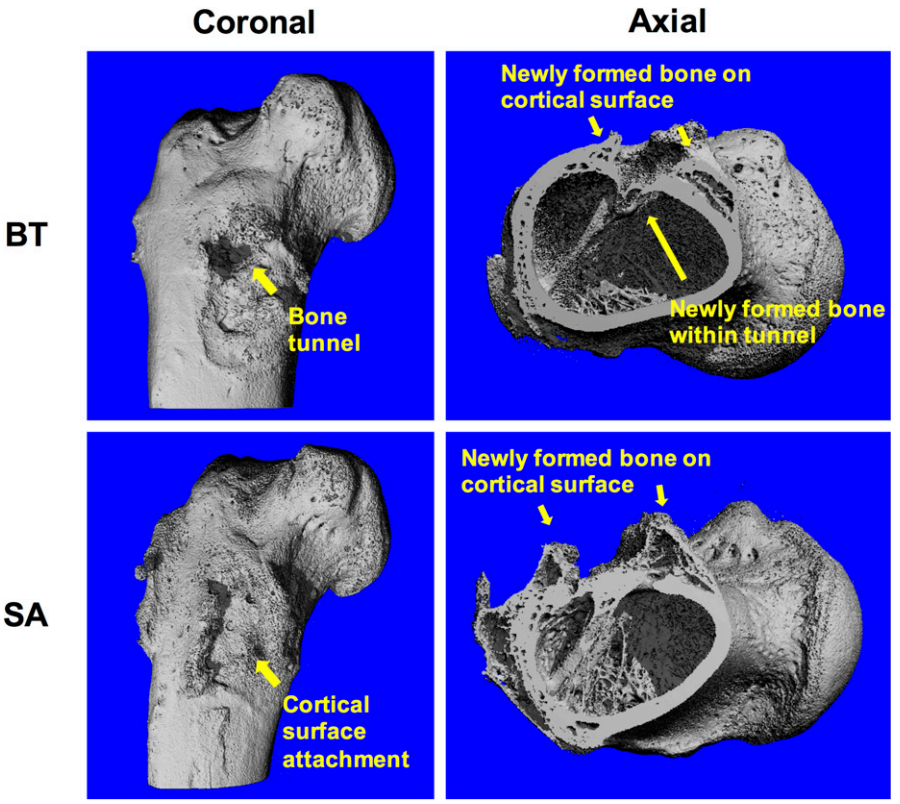

Fig. 3

Representative 3-dimensional micro-CT images of the tendon-bone attachment site for bone-tunnel fixation (BT; upper panels) and cortical surface attachment (SA; lower panels). A digital whole slide microscopic image (Cortical Surface Attachment) shows a hematoxylin and eosin (H&E)-stained slide of the cortical surface attachment group in a similar plane.

volume fraction (bone volume/total volume), apparent density (equal to mineral content/total volume), and tissue mineral density (equal to mineral content/bone volume), were performed using a global threshold of 400 mg/cm^3. Images and 3-dimensional reconstructions were evaluated with the use of Scanco μCT software (DECwindows Motif version 1.6; HP).

Histological Analysis

At the time that the animals were killed, the disarticulated humerus-tendon specimens were fixed in 10% neutral buffered formalin for 48 hours and then decalcified in Immunocal (Decal Chemical) for 72 hours. The tissues were then dehydrated with ethanol and embedded in paraffin. For the BT specimens, sections were made from the middle of the tunnel by cutting the tunnel in half lengthwise and then embedding each half. Tissues were embedded exactly perpendicular to the biceps tendon-tunnel complex to obtain an axial cross-section. For both groups, sagittal sections were made through the middle of the bicipital groove containing the tendon-cortical surface interface and then embedded. Consecutive 5-μm-thick sections were cut and stained with hematoxylin-eosin and safranin O for histological evaluation. After images viewed on a light microscope were digitally converted, ImageJ (National Institutes of Health) was used to outline and measure the thickness of the tendon-bone interface. Histomorphometric scoring was performed by 2 independent observers using a previously described scoring system based on 2 criteria: fibrocartilage zone formation and tendon bonding to adjacent tissues (Table I)[21]. The observers could not be blinded to the treatment group because of the obvious difference in the morphology of the sections.

Statistical Methods

A comparison of the modes of failure between the groups was performed with the chi-square test. Comparisons of biomechanical measurements, micro-CT measurements,

TABLE II Micro-CT Measurements of Newly Formed Bone on the Cortical Surface*

	BT†	SA†	P Value
BV (*mm^3*)	65.98 ± 15.14	65.43 ± 21.90	0.96
BV/TV (*%*)	61.00 ± 8.21	51.30 ± 9.64	0.07
AD (*mg/cm^3*)	438.44 ± 54.93	361.66 ± 60.70	0.03
TMD (*mg/cm^3*)	727.12 ± 12.51	698.59 ± 26.20	0.03

*BT = bone tunnel, SA = cortical surface attachment, BV = bone volume, BV/TV = bone volume fraction (bone volume/total volume), AD = apparent density, and TMD = tissue mineral density. †The values are given as the mean and the standard deviation.

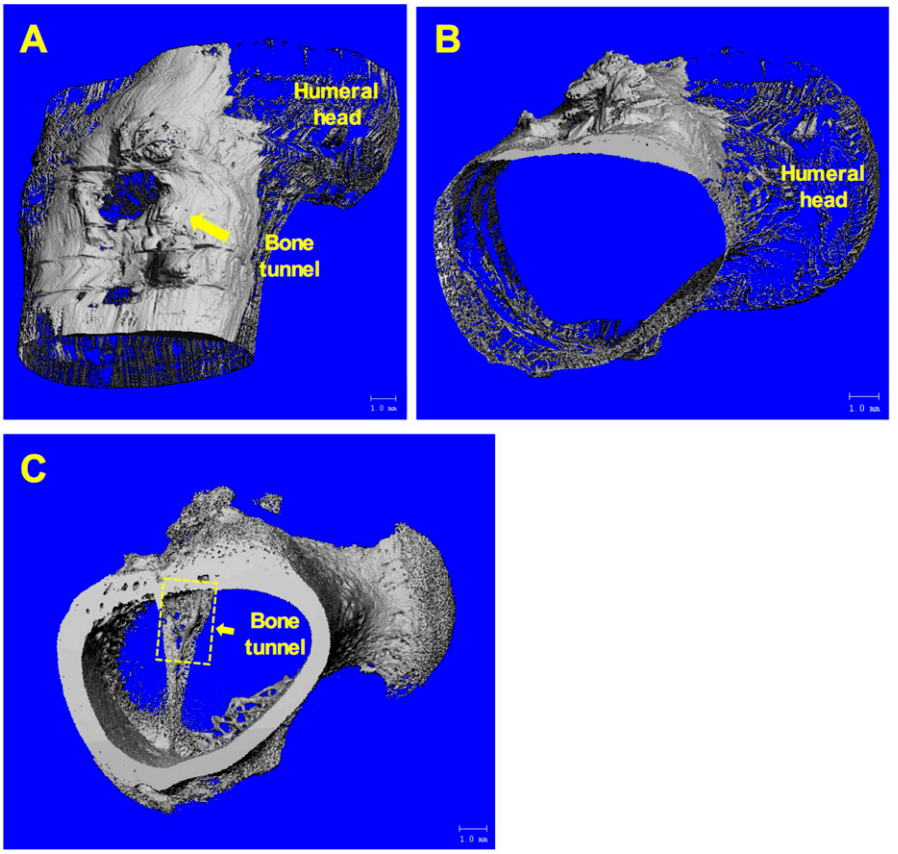

Fig. 4

Representative 3-dimensional micro-CT images of newly formed bone on the cortical surface (**Figs. 4-A and 4-B**) and within the bone tunnel (**Fig. 4-C**) in a single specimen in the bone tunnel (BT) group. On average, newly formed bone within the bone tunnel represented only 5.3% of the total new bone formation in the BT group. The digital whole slide microscopic image (Bone-Tunnel Fixation) also shows the paucity of new bone surrounding the tendon in the tunnel.

and histomorphometric scores between the groups were performed using independent-samples t tests. For each BT specimen, comparisons between micro-CT measurements of newly formed bone on the cortical surface and that within the bone tunnel were performed using paired-samples t tests. The interrater reliability of the histomorphometric scores between the 2 evaluators was assessed using the intraclass correlation coefficient (ICC 2,2). Two-tailed tests were used for all statistical analyses, with a p value of 0.05 indicating significance.

Results

Intraoperative Complications

There were no surgical complications, infections, or wound complications in the intraoperative period. One rabbit from the BT group died 3 days postoperatively from atypical bronchopneumonia. At 8 weeks, there were no gross failures (tendon pullout or rupture) at the tenodesis site.

Biomechanical Testing

We found no significant difference in the mean load to failure (and standard deviation) between the BT group (56.8 ± 28.8 N) and the SA group (55.8 ± 14.9 N) (p = 0.92). In comparison, the mean load to failure for the native biceps attachment to the supraglenoid tubercle was >100 N. We also found no significant difference in the mean stiffness between the BT group (26.3 ± 16.6 N/mm) and the SA group (32.3 ± 9.6 N/mm) (p = 0.34) (Fig. 2). Tendon pullout occurred at the bone tunnel in 8 of the BT specimens (80%), whereas failure at the tenodesis site occurred in only 2 SA specimens (20%), with the rest failing at the tendon midsubstance distal to the tenodesis site (p = 0.02).

Micro-CT Quantification of Newly Formed Bone

The mean total volume of newly formed bone was 69.3 ± 13.9 mm^3 in the BT group and 65.5 ± 21.9 mm^3 in the SA group (p = 0.70) (Fig. 3; link to the digital whole slide image: Cortical Surface Attachment). The mean total tissue mineral density of newly formed bone was 721.4 ± 10.9 mg/cm^3 in the BT group and 698.6 ± 26.2 mg/cm^3 in the SA group (p = 0.07). There were no significant associations between the total bone volume and tissue mineral density of newly formed bone and the biomechanical measurements within each specimen.

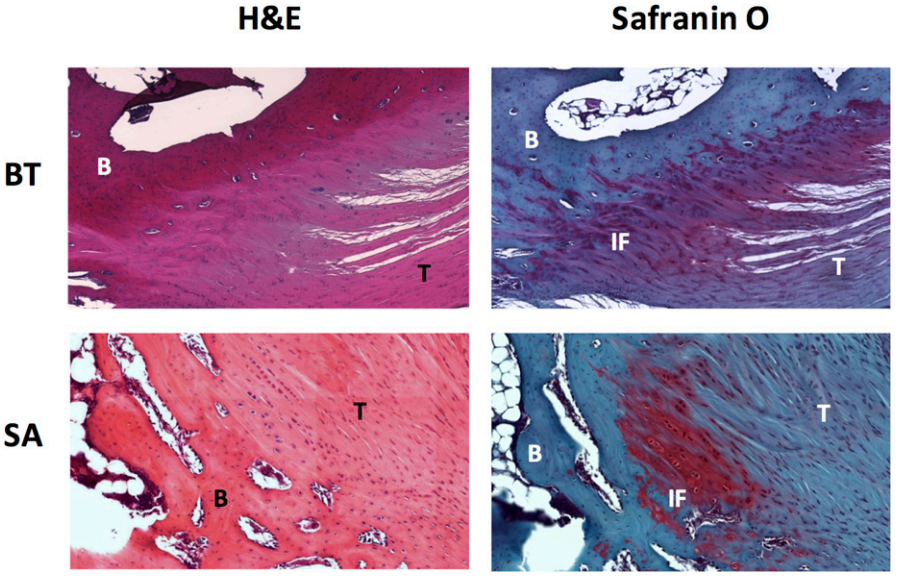

Fig. 5

Representative hematoxylin and eosin (H&E) and safranin O staining (×4) of sagittal paraffin sections through the tendon-bone interface at the cortical surface in the bone tunnel (BT) group (upper panels) and the cortical surface attachment (SA) group (lower panels) at 8 weeks. T = tendon, B = bone, and IF = fibrocartilage interface. Further analysis is possible with the digital whole slide microscopic images (Bone-Tunnel Fixation, Cortical Surface Attachment).

The mean bone volume, bone volume fraction (bone volume/total volume), apparent density, and tissue mineral density of newly formed bone on the cortical surface are shown in Table II. The 2 groups did not differ significantly with respect to the mean bone volume and bone volume fraction of newly formed bone on the cortical surface. The mean apparent density and tissue mineral density of newly formed bone on the cortical surface were higher in the BT group than in the SA group ($p = 0.03$), but these differences were small (differences of 76.8 mg/cm^3 and 28.5 mg/cm^3 for apparent density and tissue mineral density, respectively).

In the BT group, the mean bone volume and tissue mineral density of newly formed bone within the bone tunnel were 3.4 ± 1.8 mm^3 and 614.2 ± 24.9 mg/cm^3, respectively. On average, newly formed bone within the bone tunnel represented only 5.3% ± 3.4% of the total new bone formed in the BT specimens (Fig. 4; link to the digital whole slide image: Bone-Tunnel Fixation). The intraspecimen tissue mineral density of newly formed bone within the bone tunnel was significantly lower than the tissue mineral density of newly formed bone on the cortical surface ($p < 0.01$).

Histological Analysis

At 8 weeks, areas of direct tendon-bone interdigitation and early fibrocartilaginous zone formation were observed at the tendon-bone interface on the outer cortical surface in both groups (Fig. 5; links to the digital whole slide images: Bone-Tunnel Fixation; Cortical Surface Attachment). Within the tunnel in the BT specimens, minimal tendon-bone bonding was observed, with a paucity of trabecular bone in the medullary canal overall (Fig. 6). The ICC between the scores of the 2 independent observers was 0.75. The mean histomorphometric

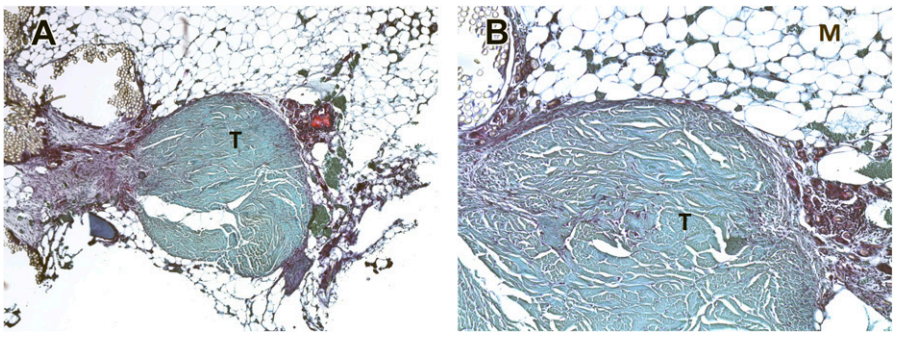

Fig. 6

Representative safranin O staining of axial sections of the tendon within the bone tunnel at 8 weeks, magnification ×4 (**Fig. 6-A**) and ×10 (**Fig. 6-B**). Minimal tendon-bone bonding is seen. T = tendon, and M = marrow.

scores were 5.7 ± 1.2 and 6.0 ± 1.6 for the BT group and 6.2 ± 1.8 and 6.2 ± 1.8 for the SA group, with no significant difference in scores between the groups.

Discussion

Previous studies have characterized the process of tendon-healing within a bone tunnel, which progresses through a zone of interposing fibrous tissue that reorganizes until final osseointegration of the tendon[22-24]. However, in the current study, we observed minimal new bone formation and tendon-bone bonding within the bone tunnel, which is consistent with that seen in rats[25]. Although new bone did form around the perimeter of the tunnel, bonding between this new bone and the intratunnel segment of tendon was infrequent and may have been limited by micromotion of the tendon. Mazzocca et al. compared the cyclic displacement of biceps tendons fixed within a bone tunnel or on the cortical surface in cadavers[4]. Although no significant differences in ultimate strength were found between techniques, greater cyclic displacement was noted for bone-tunnel fixation. Motion of the tendon within a bone tunnel delays healing at the tendon-bone interface[26], and without a robust interference fit between the tendon and cancellous bone, a greater degree of cyclic motion is to be expected. In the current study, the size of the long head of the biceps tendon and the location of the musculotendinous junction were likely factors in the amount of tendon motion within the bone tunnel. While the diameter of the bone tunnel remained consistent (2.4 mm), the tendon diameter and the proximal start of the musculotendinous junction were heterogeneous among the rabbits, leading to variability in the "tightness" of the tendon within the tunnel. Additionally, in quadrupedal animal models, joint motion and loading on the healing tendon are difficult to control because of the inability to reliably immobilize the extremity or restrict weight-bearing. This is likely reflected by the higher variability in failure loads observed in the BT group.

Although tendon-healing within the bone tunnel was minimal, healing on the outer cortical surface was similar between the groups. Prior in vivo investigations of tendon-healing within a bone tunnel frequently have overlooked the concurrent healing that occurs outside, at the tunnel exit site. We believe that this is partly because of the primary utilization of anterior cruciate ligament reconstruction models in the majority of tendon-to-bone healing studies, in which the graft is placed in-line with the intra-articular tunnel[23,26-29], as well as the seeming belief that tendon-healing within the tunnel is the most important determinant of final construct strength[13,22,24]. To our knowledge, the only other study to directly compare the tendon-healing profiles between bone tunnel and cortical surface fixation was performed by Silva et al.[13], who examined tendon-to-bone healing in a canine model of flexor digitorum repair. Better maturation of the tendon-bone interface was reported in surface repairs compared with tunnel repairs; however, for the latter group, the authors did not specifically examine the healing outside the tunnel. Additionally, consistent with the results of our study, bone mineral density and trabecular bone volume were not different between the groups, although the authors computed these measurements from the entire distal phalanx rather than just from newly formed bone. In contrast with our biomechanical results, the authors reported that bone tunnel repairs had a 38% lower ultimate strength compared with surface repairs after 21 days. Although we did not observe any difference in mean failure loads between our experimental groups, our testing was limited by premature failure of the biceps tendon at the midsubstance in the majority of the SA specimens. This may be a result of stress risers at the suture-tendon interface, leading to weakening of the tendon distally. The tenodesis site in these SA specimens may have been stronger than that in BT specimens, although we cannot confirm this. It is important to note that 3 weeks for a large canine model represents an earlier phase of healing than does 8 weeks for our smaller rabbit model. Nevertheless, both studies effectively examined an early-to-middle phase of healing[30]. While our results may have implications for the early-to-middle rehabilitation period, a comparison of fixation techniques after the final maturation phase of healing is ultimately needed to determine which technique facilitates a stronger biological construct.

The supposed benefits of tendon-to-cancellous-bone healing were not confirmed through the results of our study. Although tendons placed within a tunnel theoretically increases their exposure to marrow-derived stem cells, thereby enhancing osseointegration[8,9], tendons affixed to the cortical surface can be exposed to a similar milieu from the periosteum or unicortical drill holes[31,32]. A previous report of rotator cuff healing in a goat model noted no histological differences between repairs in which the tendon was attached to cortical bone versus a cancellous trough at 6 and 12 weeks[33]. Additionally, although greater tendon-bone contact within a tunnel is thought to increase the total area of biological integration, the majority of healing in our BT group occurred outside the tunnel, at the cortical surface.

The results of the present study have several potential clinical implications. Our biomechanical and histological data suggest that cortical fixation of the long head of the biceps tendon exhibits satisfactory tendon-to-bone healing that is similar to previous descriptions of healing of other tendons to cortical bone[13,33,34]. Cortical surface fixation can be accomplished with the use of suture anchors or small cortical buttons, which involve drilling smaller holes compared with the larger hole needed to accommodate the width of a docked biceps tendon. Creation of a larger cortical hole can generate stress risers in the proximal humeral shaft, risking a fracture[11,12]. Additionally, cortical fixation avoids the need for an interference screw and its associated potential complications, including tendon stripping at the screw-tendon interface and cyst formation from the use of bioabsorbable material[18,35]. Ultimately, both techniques can facilitate good tendon-to-bone healing, and surgeon preference will likely dictate the decision to use one method over the other. ■

NOTE: The authors thank Yusuke Nakagawa, MD, PhD, for his assistance with the animal surgeries.

Hongbo Tan, MD, PhD[1]
Dean Wang, MD[1]
Amir H. Lebaschi, MD[1]
Ian D. Hutchinson, MD[1]
Liang Ying, BS[1]
Xiang-Hua Deng, MD[1]
Scott A. Rodeo, MD[1]
Russell F. Warren, MD[1]

[1]Laboratory for Joint Tissue Repair and Regeneration, Orthopaedic Soft Tissue Research Program (H.T., D.W., A.H.L., I.D.H., L.Y., X.-H.D., S.A.R., and R.F.W.) and Sports Medicine and Shoulder Service (D.W., S.A.R., and R.F.W.), Hospital for Special Surgery, New York, NY

E-mail address for D. Wang: deanwangmd@gmail.com

ORCID iD for D. Wang: 0000-0002-3005-1154

References

1. Ahrens PM, Boileau P. The long head of biceps and associated tendinopathy. J Bone Joint Surg Br. 2007 Aug;89(8):1001-9.

2. Boileau P, Ahrens PM, Hatzidakis AM. Entrapment of the long head of the biceps tendon: the hourglass biceps—a cause of pain and locking of the shoulder. J Shoulder Elbow Surg. 2004 May-Jun;13(3):249-57.

3. McDonald LS, Dewing CB, Shupe PG, Provencher MT. Disorders of the proximal and distal aspects of the biceps muscle. J Bone Joint Surg Am. 2013 Jul 3;95 (13):1235-45.

4. Mazzocca AD, Bicos J, Santangelo S, Romeo AA, Arciero RA. The biomechanical evaluation of four fixation techniques for proximal biceps tenodesis. Arthroscopy. 2005 Nov;21(11):1296-306.

5. Richards DP, Burkhart SS. A biomechanical analysis of two biceps tenodesis fixation techniques. Arthroscopy. 2005 Jul;21(7):861-6.

6. Buchholz A, Martetschläger F, Siebenlist S, Sandmann GH, Hapfelmeier A, Lenich A, Millett PJ, Stöckle U, Elser F. Biomechanical comparison of intramedullary cortical button fixation and interference screw technique for subpectoral biceps tenodesis. Arthroscopy. 2013 May;29(5):845-53. Epub 2013 Mar 7.

7. Tashjian RZ, Henninger HB. Biomechanical evaluation of subpectoral biceps tenodesis: dual suture anchor versus interference screw fixation. J Shoulder Elbow Surg. 2013 Oct;22(10):1408-12. Epub 2013 Feb 15.

8. Lim JK, Hui J, Li L, Thambyah A, Goh J, Lee EH. Enhancement of tendon graft osteointegration using mesenchymal stem cells in a rabbit model of anterior cruciate ligament reconstruction. Arthroscopy. 2004 Nov;20(9):899-910.

9. Soon MY, Hassan A, Hui JH, Goh JC, Lee EH. An analysis of soft tissue allograft anterior cruciate ligament reconstruction in a rabbit model: a short-term study of the use of mesenchymal stem cells to enhance tendon osteointegration. Am J Sports Med. 2007 Jun;35(6):962-71. Epub 2007 Mar 30.

10. Dovan TT, Gelberman RH, Kusano N, Calcaterra M, Silva MJ. Zone I flexor digitorum profundus repair: an ex vivo biomechanical analysis of tendon to bone repair in cadavera. J Hand Surg Am. 2005 Mar;30(2):258-66.

11. Sears BW, Spencer EE, Getz CL. Humeral fracture following subpectoral biceps tenodesis in 2 active, healthy patients. J Shoulder Elbow Surg. 2011 Sep;20(6): e7-11. Epub 2011 May 24.

12. Dein EJ, Huri G, Gordon JC, McFarland EG. A humerus fracture in a baseball pitcher after biceps tenodesis. Am J Sports Med. 2014 Apr;42(4):877-9. Epub 2014 Feb 5.

13. Silva MJ, Thomopoulos S, Kusano N, Zaegel MA, Harwood FL, Matsuzaki H, Havlioglu N, Dovan TT, Amiel D, Gelberman RH. Early healing of flexor tendon insertion site injuries: tunnel repair is mechanically and histologically inferior to surface repair in a canine model. J Orthop Res. 2006 May;24(5):990-1000.

14. Park JS, Kim SH, Jung HJ, Lee YH, Oh JH. A prospective randomized study comparing the interference screw and suture anchor techniques for biceps tenodesis. Am J Sports Med. 2017 Feb;45(2):440-8. Epub 2016 Oct 22.

15. Millett PJ, Sanders B, Gobezie R, Braun S, Warner JJ. Interference screw vs. suture anchor fixation for open subpectoral biceps tenodesis: does it matter? BMC Musculoskelet Disord. 2008 Sep 15;9:121.

16. Mazzocca AD, Cote MP, Arciero CL, Romeo AA, Arciero RA. Clinical outcomes after subpectoral biceps tenodesis with an interference screw. Am J Sports Med. 2008 Oct;36(10):1922-9. Epub 2008 Aug 12.

17. Virk MS, Nicholson GP. Complications of proximal biceps tenotomy and tenodesis. Clin Sports Med. 2016 Jan;35(1):181-8. Epub 2015 Sep 28.

18. Koch BS, Burks RT. Failure of biceps tenodesis with interference screw fixation. Arthroscopy. 2012 May;28(5):735-40.

19. Abtahi AM, Granger EK, Tashjian RZ. Complications after subpectoral biceps tenodesis using a dual suture anchor technique. Int J Shoulder Surg. 2014 Apr;8 (2):47-50.

20. Nho SJ, Reiff SN, Verma NN, Slabaugh MA, Mazzocca AD, Romeo AA. Complications associated with subpectoral biceps tenodesis: low rates of incidence following surgery. J Shoulder Elbow Surg. 2010 Jul;19(5):764-8. Epub 2010 May 14.

21. Zhou Y, Zhang J, Yang J, Narava M, Zhao G, Yuan T, Wu H, Zheng N, Hogan MV, Wang JH. Kartogenin with PRP promotes the formation of fibrocartilage zone in the tendon-bone interface. J Tissue Eng Regen Med. 2017 Jan 27. Epub 2017 Jan 27.

22. Rodeo SA, Arnoczky SP, Torzilli PA, Hidaka C, Warren RF. Tendon-healing in a bone tunnel. A biomechanical and histological study in the dog. J Bone Joint Surg Am. 1993 Dec;75(12):1795-803.

23. Grana WA, Egle DM, Mahnken R, Goodhart CW. An analysis of autograft fixation after anterior cruciate ligament reconstruction in a rabbit model. Am J Sports Med. 1994 May-Jun;22(3):344-51.

24. Liu SH, Panossian V, al-Shaikh R, Tomin E, Shepherd E, Finerman GA, Lane JM. Morphology and matrix composition during early tendon to bone healing. Clin Orthop Relat Res. 1997 Jun;339:253-60.

25. Urch E, Taylor SA, Ramkumar PN, Doty SB, White AE, Delos D, Shorey ME, O'Brien SJ. Biceps tenodesis: a comparison of tendon-to-bone and tendon-to-tendon healing in a rat model. J Shoulder Elbow Surg. 2016;25(6):e179-80.

26. Rodeo SA, Kawamura S, Kim HJ, Dynybil C, Ying L. Tendon healing in a bone tunnel differs at the tunnel entrance versus the tunnel exit: an effect of graft-tunnel motion? Am J Sports Med. 2006 Nov;34(11):1790-800. Epub 2006 Jul 21.

27. Weiler A, Hoffmann RF, Bail HJ, Rehm O, Südkamp NP. Tendon healing in a bone tunnel. Part II: histologic analysis after biodegradable interference fit fixation in a model of anterior cruciate ligament reconstruction in sheep. Arthroscopy. 2002 Feb;18(2):124-35.

28. Weiler A, Peine R, Pashmineh-Azar A, Abel C, Südkamp NP, Hoffmann RF. Tendon healing in a bone tunnel. Part I: biomechanical results after biodegradable interference fit fixation in a model of anterior cruciate ligament reconstruction in sheep. Arthroscopy. 2002 Feb;18(2):113-23.

29. Blickenstaff KR, Grana WA, Egle D. Analysis of a semitendinosus autograft in a rabbit model. Am J Sports Med. 1997 Jul-Aug;25(4):554-9.

30. Karaoglu S, Celik C, Korkusuz P. The effects of bone marrow or periosteum on tendon-to-bone tunnel healing in a rabbit model. Knee Surg Sports Traumatol Arthrosc. 2009 Feb;17(2):170-8. Epub 2008 Oct 22.

31. O'Driscoll SW, Recklies AD, Poole AR. Chondrogenesis in periosteal explants. An organ culture model for in vitro study. J Bone Joint Surg Am. 1994 Jul;76 (7):1042-51.

32. Hopper RA, Zhang JR, Fourasier VL, Morova-Protzner I, Protzner KF, Pang CY, Forrest CR. Effect of isolation of periosteum and dura on the healing of rabbit calvarial inlay bone grafts. Plast Reconstr Surg. 2001 Feb;107(2):454-62.

33. St Pierre P, Olson EJ, Elliott JJ, O'Hair KC, McKinney LA, Ryan J. Tendon-healing to cortical bone compared with healing to a cancellous trough. A biomechanical and histological evaluation in goats. J Bone Joint Surg Am. 1995 Dec;77(12):1858-66.

34. Boyer MI, Harwood F, Ditsios K, Amiel D, Gelberman RH, Silva MJ. Two-portal repair of canine flexor tendon insertion site injuries: histologic and immunohistochemical characterization of healing during the early postoperative period. J Hand Surg Am. 2003 May;28(3):469-74.

35. Barber FA. Complications of biodegradable materials: anchors and interference screws. Sports Med Arthrosc. 2015 Sep;23(3):149-55.